Semnan University

Journal of Heat and Mass Transfer Research

Journal homepage: http://jhmtr.journals.semnan.ac.ir

# Effects of variations in magnetic Reynolds number on magnetic field distribution in electrically conducting fluid under magnetohydrodynamic natural convection

Mohsen Pirmohammadi

Department of Mechanical Engineering, Pardis Branch , Islamic Azad University, Pardis, Iran

**PAPER INFO**

**History:**

Submitted 2016-12-15
Revised 2017-10-07
Accepted 2017-10-12

**Keywords**:

Magnetic Reynolds; number;
Natural convection;
Magnetic field

**A B S T R A C T**

This study numerically investigated the effects of variations in magnetic Reynolds number on magnetic field distribution in an enclosure under natural convection heat transfer. The investigated geometry was a two-dimensional enclosure with a hot left wall, a cold right wall, and adiabatic top and bottom walls. The fluid was molten sodium with Pr=0.01. Natural convection heat transfer at a Rayleigh number of 105 and magnetic Reynolds numbers (Rem) of 10–1, 10–3, and 10–5 was considered in the analysis. The governing equations adopted were continuum, momentum, energy, and magnetic induction equations, which were solved concurrently using the finite volume method. For the coupling of velocity and pressure, the revised semi-implicit method for pressure linked equations algorithm was employed. Results showed that under a high magnetic Reynolds number, the non-dimensional magnetic fields in the X and Y directions were approximately constant because the diffusion of the magnetic potential was greater than the advection of such potential. As the magnetic Reynolds number increased, however, the magnetic field in the enclosure reached a magnitude unequal to that of the applied magnetic field, exhibited inconstancy, and increased to a value that deviated from 1. Thus, the Rem=10–1 under a non-dimensional magnetic field increased from 0.09 to 6.6 in the X direction and from –1.164 to 4.05 in Y the direction.



DOI: 10.22075/jhmtr.2017.1503.1100

## 1. Introduction

The free convection heat transfer of electrically conducting fluids in enclosures has been the subject of a considerable number of theoretical, experimental, and numerical investigations because of its importance in many technological applications, such as use in liquid metal blankets for reactors. Another important application of the aforementioned process is crystal growth in the industrial production of semiconductors. This particular application has been explored in a number of works. Oreper and Szekely [1], for example, showed that a magnetic field suppresses natural convection currents and that magnetic field strength is a critical factor for crystal formation. Hadid et al. [2] probed into the effects of a strong vertical magnetic field on convection and segregation in vertical Bridgeman crystal growth. Bessaih et al. [3] numerically examined the effects of the electric conductivity of walls and the direction of a magnetic field on gallium flow. The authors found a considerable reduction in convection intensity as the magnetic field increases.

Ciofalo and Cricchio [4] considered the MHD natural convection of liquid Pb–17Li in a cubical cavity with a uniform volumetric heat source and an induced current that significantly stretches to the walls normal to the applied magnetic field flux. Piazza and Ciofalo [5, 6] developed a simple wall boundary

Corresponding Author : Department of Mechanical Engineering, Pardis Branch , Islamic Azad University, Pardis, Iran
Email: Pirmohamadi@pardisiau.ac.ir

condition to solve electromagnetism in a cavity without allocating real grid points to electrically conducting walls. Pirmohammadi et al. [7] numerically studied natural convection flow in the presence of a magnetic field in a tilted enclosure heated from below and filled with liquid gallium. The authors found that at a given inclination angle, convection heat transfer decreases when magnetic field intensity increases. Pirmohammadi et al. [8] studied the effects of a magnetic field on buoyancy-driven convection in a differentially heated square enclosure. The researchers showed that the heat transfer mechanisms and flow characteristics in the enclosure depend strongly on both the strength of the magnetic field and the Rayleigh number. They concluded that a magnetic field considerably decreases the average Nusselt number.

An extensive study of mixed convection was conducted by Selimefendigil et al. [11] for various geometries. Heidary et al. [12] numerically investigated the laminar flow and convective heat transfer of Cu-water nanofluid in a channel subjected to a uniform magnetic field. The authors revealed that the thickness of the thermal boundary layer increases with the addition of nanoparticles to pure fluid. Applying a magnetic field, however, thins the boundary layer because of the increase in velocity gradient near walls. Seth et al. [13] delved into the combined free and forced convection Couette–Hartmann flow of a viscous, incompressible, and electrically conducting fluid. The fluid was placed in a rotating channel with arbitrary conducting walls, and flow was examined under the presence of the Hall current. Makinde et al. [14] investigated the steady flow and heat transfer of an electrically conducting fluid with variable viscosity and electrical conductivity between two parallel plates in the presence of a transverse magnetic field.

In most of the above-mentioned studies, mathematical and numerical methods were intended to determine the influence of any combination of Grashof, Reynolds, Prandtl, and Hartmann numbers on flow and heat transfer. A technique common to these studies was the simplification of the magnetic induction equation on the basis of low Reynolds approximation [15, 16]. The dimensionless magnetic Reynolds number ($\mathrm{Re}_m = \sigma\mu_0 v$) of flow represents the ratio of advection to diffusion in a magnetic field. At $\mathrm{Re}_m \ll 1$, advection is relatively unimportant, and a magnetic field thus tends to relax toward a purely diffusive state. This relaxation is determined by boundary conditions rather than flow; consequently, fluid motion has no influence on magnetic field distribution.

In this work, a simulation of magneto-convective flow was carried out inside a square cavity. The purpose of the current study was to numerically solve full magnetic induction, continuum, momentum, and energy equations to investigate the effect of the magnetic Reynolds number on the magnetic field distribution and temperature and velocity profiles.

## 2. Basic Equations

The schematic of the examined enclosure is depicted in Fig. 1. The cavity is differentially heated; the left and right walls are isothermal at $T_H$ and $T_C$, respectively ($T_H > T_C$); and the horizontal walls are adiabatic. A magnetic field was applied in the X direction.

The governing equations used in this research are based on the conservation laws of mass, momentum, energy, and induction equations. The governing equations are provided below:

$$\frac{\partial u}{\partial x} + \frac{\partial v}{\partial y} = 0 \tag{1}$$

$$\rho\left(u\frac{\partial u}{\partial x} + v\frac{\partial u}{\partial y}\right) = -\frac{\partial P}{\partial x} + \mu\left(\frac{\partial^2 u}{\partial x^2} + \frac{\partial^2 u}{\partial y^2}\right) - \frac{1}{\mu_0}\left(\frac{\partial B_y}{\partial x} - \frac{\partial B_x}{\partial y}\right)B_y \tag{2}$$

$$\rho\left(u\frac{\partial v}{\partial x} + v\frac{\partial v}{\partial y}\right) = -\frac{\partial P}{\partial y} + \mu\left(\frac{\partial^2 v}{\partial x^2} + \frac{\partial^2 v}{\partial y^2}\right) + \rho g\beta(T - T_c) + \frac{1}{\mu_0}\left(\frac{\partial B_y}{\partial x} - \frac{\partial B_x}{\partial y}\right)B_X \tag{3}$$

$$\rho Cp\left(u\frac{\partial T}{\partial x} + v\frac{\partial T}{\partial y}\right) = k\left(\frac{\partial^2 T}{\partial x^2} + \frac{\partial^2 T}{\partial y^2}\right) \tag{4}$$

$$u\frac{\partial B_x}{\partial x} + v\frac{\partial B_x}{\partial y} = B_x\frac{\partial u}{\partial x} + B_y\frac{\partial u}{\partial y} + \frac{1}{\sigma\mu_0}\left(\frac{\partial^2 B_x}{\partial x^2} + \frac{\partial^2 B_x}{\partial y^2}\right) \tag{5}$$

$$u\frac{\partial B_y}{\partial x} + v\frac{\partial B_y}{\partial y} = B_x\frac{\partial v}{\partial x} + B_y\frac{\partial v}{\partial y} + \frac{1}{\sigma\mu_0}\left(\frac{\partial^2 B_y}{\partial x^2} + \frac{\partial^2 B_y}{\partial y^2}\right) \tag{6}$$

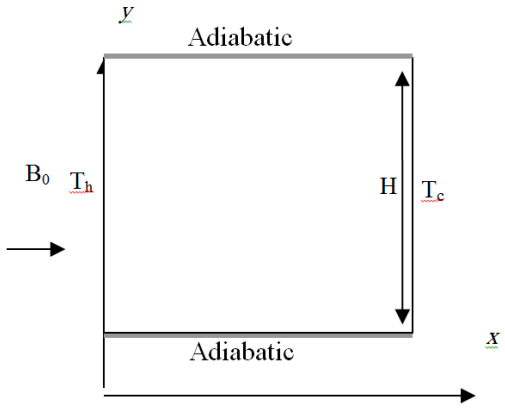


Fig. 1. Geometry and coordinates of cavity configuration with magnetic effect

More details regarding Equations (5) and (6) can be found in [17]. In the equations above, u and v are velocity components, p denotes the pressure, T is the temperature, $\rho$ represents the density, g is the gravitational acceleration, $\mu$ is the viscosity, $\beta$ is the coefficient of thermal expansion, $B_x$ stands for the magnetic field in the X direction, and $B_y$ represents the magnetic field in the Y direction. Moreover, k pertains to the thermal conductivity, Cp is the specific heat capacity, $\sigma$ is the electrical conductivity, and $\mu_0$ denotes the magnetic permeability.

3. The dimensionless variables included in the analysis are defined thus:

$$X = \frac{x}{H}\ , Y = \frac{y}{H}\ , U = \frac{\rho CpuH}{k}\ , V = \frac{\rho CpvH}{k}\ ,$$

$$P = \frac{\rho Cp^2 pH^2}{k^2}, \theta = \frac{T - T_C}{T_H - T_C}\ ,\ \mathrm{Re_m} = \sigma\mu_0 v\ ,$$

$$B_x^* = \frac{B_x}{B_0},\ B_y^* = \frac{B_y}{B_0},\quad \mathrm{Pr} = \frac{k}{\rho c_p} \tag{7}$$

$$, Ra = \frac{c_p g\beta(T_h - T_c)H^3}{k\mu}, Ha = B_0 H\sqrt{\frac{\sigma}{\mu}}$$

On the basis of these variables, the governing equations are expressed in dimensionless form as follows:

$$\frac{\partial U}{\partial X} + \frac{\partial V}{\partial Y} = 0 \tag{8}$$

$$\mathrm{U}\frac{\partial \mathrm{U}}{\partial \mathrm{X}} + \mathrm{V}\frac{\partial \mathrm{U}}{\partial \mathrm{Y}} = -\frac{\partial \mathrm{P}}{\partial \mathrm{X}} + \mathrm{Pr}\left(\frac{\partial^2 U}{\partial \mathrm{X}^2} + \frac{\partial^2 U}{\partial \mathrm{Y}^2}\right) - Ha^2 \frac{\mathrm{Pr}^2}{\mathrm{Re}_m} B_y^* \left(\frac{\partial \mathrm{B}_y^*}{\partial \mathrm{X}} - \frac{\partial \mathrm{B}_x^*}{\partial \mathrm{Y}}\right) \tag{9}$$

$$\mathrm{U}\frac{\partial \mathrm{V}}{\partial \mathrm{X}} + \mathrm{V}\frac{\partial \mathrm{V}}{\partial \mathrm{Y}} = -\frac{\partial \mathrm{P}}{\partial \mathrm{Y}} + \mathrm{Pr}\left(\frac{\partial^2 V}{\partial \mathrm{X}^2} + \frac{\partial^2 V}{\partial \mathrm{Y}^2}\right) + \mathrm{RaPr}\theta + Ha^2 \frac{\mathrm{Pr}^2}{\mathrm{Re}_m} B_x^* \left(\frac{\partial \mathrm{B}_y^*}{\partial \mathrm{X}} - \frac{\partial \mathrm{B}_x^*}{\partial \mathrm{Y}}\right) \tag{10}$$

$$U\frac{\partial \theta}{\partial X} + V\frac{\partial \theta}{\partial Y} = \frac{\partial^2 \theta}{\partial X^2} + \frac{\partial^2 \theta}{\partial X^2} \tag{11}$$

$$\mathrm{U}\frac{\partial \mathrm{B}_x^*}{\partial \mathrm{X}} + \mathrm{V}\frac{\partial \mathrm{B}_x^*}{\partial \mathrm{Y}} = \mathrm{B}_x^*\frac{\partial \mathrm{U}}{\partial \mathrm{X}} + \mathrm{B}_y^*\frac{\partial \mathrm{U}}{\partial \mathrm{Y}} + \frac{\mathrm{Pr}}{\mathrm{Re}_m}\left(\frac{\partial^2 \mathrm{B}_x^*}{\partial \mathrm{X}^2} + \frac{\partial^2 \mathrm{B}_x^*}{\partial \mathrm{Y}^2}\right) \tag{12}$$

$$\mathrm{U}\frac{\partial \mathrm{B}_y^*}{\partial \mathrm{X}} + \mathrm{V}\frac{\partial \mathrm{B}_y^*}{\partial \mathrm{Y}} = \mathrm{B}_x^*\frac{\partial \mathrm{V}}{\partial \mathrm{X}} + \mathrm{B}_y^*\frac{\partial \mathrm{V}}{\partial \mathrm{Y}} + \frac{\mathrm{Pr}}{\mathrm{Re}_m}\left(\frac{\partial^2 \mathrm{B}_y^*}{\partial \mathrm{X}^2} + \frac{\partial^2 \mathrm{B}_y^*}{\partial \mathrm{Y}^2}\right) \tag{13}$$

To calculate the magnetic field instead of solving Equations (12) and (13), we can use the magnetic potential vector ($\vec{A}$) as follows:

$$\vec{\mathrm{B}} = \nabla \times \vec{\mathrm{A}} \tag{14}$$

$$\mathrm{B_x} = \frac{\partial \mathrm{A_z}}{\partial \mathrm{Y}}, \mathrm{B_y} = -\frac{\partial \mathrm{A_z}}{\partial \mathrm{X}} = 0, \mathrm{B_z} = \frac{\partial \mathrm{A_z}}{\partial \mathrm{Z}} = 0 \tag{15}$$

Thus, Equations (12) and (13) are converted into Equation (15) in the following manner:

$$\mathrm{U}\frac{\partial \mathrm{A}}{\partial \mathrm{X}} + \mathrm{V}\frac{\partial \mathrm{A}}{\partial \mathrm{Y}} = \frac{\mathrm{Pr}}{\mathrm{Re}_m}\left(\frac{\partial^2 \mathrm{A}}{\partial \mathrm{X}^2} + \frac{\partial^2 \mathrm{A}}{\partial \mathrm{Y}^2}\right) \tag{16}$$

The boundary conditions are

$$\mathrm{A} = \mathrm{Y}, \mathrm{B_x} = 1, \frac{\partial \mathrm{B_y}}{\partial \mathrm{X}} = 0 \text{ at } \mathrm{X} = 0 \tag{17}$$

$$\mathrm{A} = \mathrm{Y}, \mathrm{B_x} = 1, \frac{\partial \mathrm{B_y}}{\partial \mathrm{X}} = 0 \text{ at } \mathrm{X} = 1 \tag{18}$$

$$\mathrm{A} = 0, \mathrm{B_y} = 0, \frac{\partial \mathrm{B_x}}{\partial \mathrm{Y}} = 0 \text{ at } \mathrm{Y} = 0 \tag{19}$$

$$\mathrm{A} = 1, \mathrm{B_y} = 0, \frac{\partial \mathrm{B_x}}{\partial \mathrm{Y}} = 0 \text{ at } \mathrm{Y} = 1 \tag{20}$$

$$\mathrm{U\ \&\ V = 0 \text{ at all walls}} \quad (\mathrm{X} = 0, \mathrm{X} = 1, \mathrm{Y} = 0, \mathrm{Y} = 1) \tag{21}$$

$$\theta(0, Y) = 1, \theta(1, Y) = 0, \left.\frac{\partial \theta}{\partial Y}\right|_{Y=0} = 0, \left.\frac{\partial \theta}{\partial Y}\right|_{Y=1} = 0 \tag{22}$$

## 4. Numerical Procedures

The governing equations associated with the boundary conditions were solved numerically using the control volume-based finite volume method. The hybrid scheme, which is a combination of the central difference and upwind schemes, was used to discretize convection terms. A staggered grid system, in which velocity components are stored midway between scalar storage locations, was also employed. The well-known revised semi-implicit method for pressure linked equations algorithm was adopted in coupling the velocity field and pressure in the momentum equations. The solution of the fully coupled discretized equations was iteratively obtained using the tri-diagonal matrix algorithm. The values of residuals were checked on the basis of physical variables, such

as temperature, pressure, and velocity. Convergence was considered achieved when the summation of residuals was less than $10^{-4}$, as was the case for most of the dependent variables. Simulations were conducted with cell numbers ranging from 31×31 to 61×61 at a Rayleigh number (Ra) of $10^5$. Fig. 2 shows the grid distributions of the cavity.

## 5. Results and Discussion

To verify the accuracy of the numerical technique used to solve the problem considered in this work, a simulation of magneto-convective flow was carried out; the examined structure was a square enclosure with a horizontal temperature gradient and was simulated in the presence of the magnetic field reported by Sarris [18]. Fig. 3 plots the streamlines and isotherms of the solution derived in the current research and the results obtained by Sarris for Ra=7×10$^5$, Ha=100, and Pr=0.7.

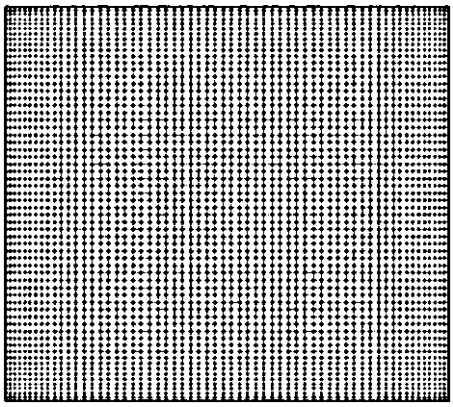

Fig. 2. Grid distributions of the cavity

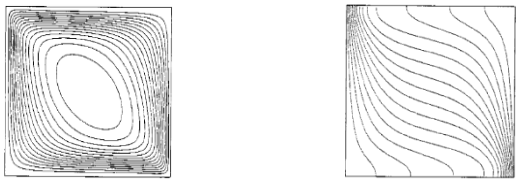

$|\psi_{\max}| = 7.23$ $\quad$ $\overline{Nu} = 3.20$

(a) Sarris's work [18]

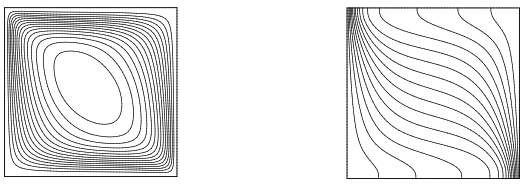

$|\psi_{\max}| = 7.10$ $\quad$ $\overline{Nu} = 3.174$

(b) Present study

Fig. 3. Comparison of isotherms and streamlines in the present work and Sarris's study at Ra=7×10$^5$ and Ha=100

In the comparison of results, the magnetic field induced by the motion of the electrically conducting fluid was disregarded. Our findings showed good agreement with those of Sarris. The relative errors in the average Nusselt number and the maximum absolute value of the stream function of Sarris work [18] and the present model were 0.8% and 1.8%, respectively. In the current research, three magnetic Reynolds numbers, namely, $10^{-1}$, $10^{-3}$, and $10^{-5}$, were adopted. The fluid used was liquid sodium with Pr=0.01 and Ra=$10^5$.

Fig. 4 shows the contours of A, $B_x$, and $B_y$ at $Re_m=10^{-5}$ and Ha=80. As expected, because the magnetic field was very small, the magnetic potential from the left to the right sides of the cavity diffused, and its quantity remained identical to that introduced into the boundary conditions. Fluid flow did not affect the applied magnetic field. Variables $B_x$ and By were calculated on the basis of the gradient of A; thus, they were constant in the entire cavity. Specifically, $B_x$ was approximately equal to 1, and $B_y$ was equal to 0. The magnetic field in the cavity was preserved.

Fig. 5 illustrates the contours of A, $B_x$, and $B_y$ at $Re_m=10^{-3}$ and Ha=80. Given that the $Re_m$ was small, the ratio of the diffusion of the magnetic potential to its advection was large. Consequently, the contours of A were approximately horizontal, and $B_x$ and $B_y$ in the cavity were constant. The maximum deviation of $B_x$ from 1 was 2.73%, and the maximum deviation of $B_y$ from 0 was 9.19%.

The contours of A, $B_x$, and $B_y$ at $Re_m=10^{-1}$ and Ha=80 are presented in Fig. 6. The advection of the magnetic potential was greater than its diffusion, thereby generating horizontal contours. The magnetic field was unequal to the applied magnetic field and was inconstant in the cavity. The magnetic field in the X direction ($B_x$) therefore varied from 0.55 to 6.6, and the magnetic field in the Y direction ($B_y$) varied from –1.164 to 4.05. The concentration of the $B_x$ contours near the horizontal walls was greater than that near the vertical walls. The magnetic field was stronger near the adiabatic walls. Furthermore, the concentration of the $B_y$ contours near the vertical walls was higher than that near the horizontal walls.

The advection of the magnetic potential was greater than its diffusion, thereby producing non-horizontal contours. The magnetic field was unequal to the applied magnetic field and was inconstant in the cavity. As a result, the magnetic field in the X direction ($B_x$) varied from 0.55 to 6.6, and the magnetic field in the Y direction ($B_y$) varied from –1.164 to 4.05. The concentration of the $B_x$ contours near the horizontal walls was higher than that near the vertical walls. The magnetic field was stronger near the adiabatic walls. The concentration of the $B_y$ contours near the vertical walls was greater than that near the horizontal walls.

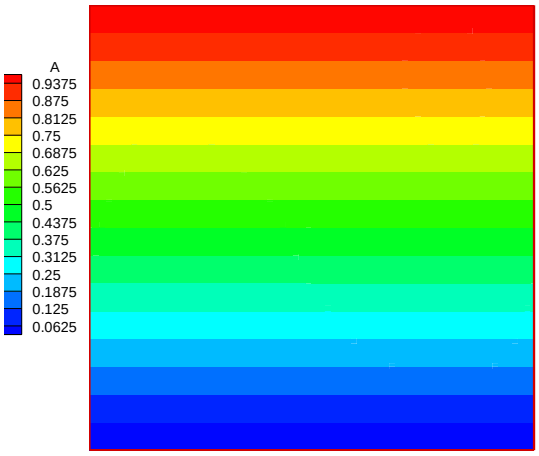


(a)

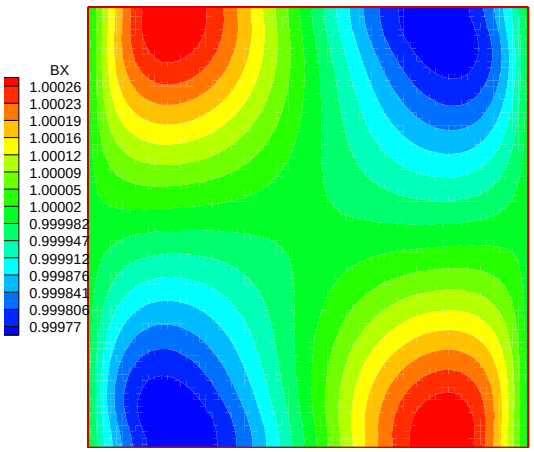


(b)

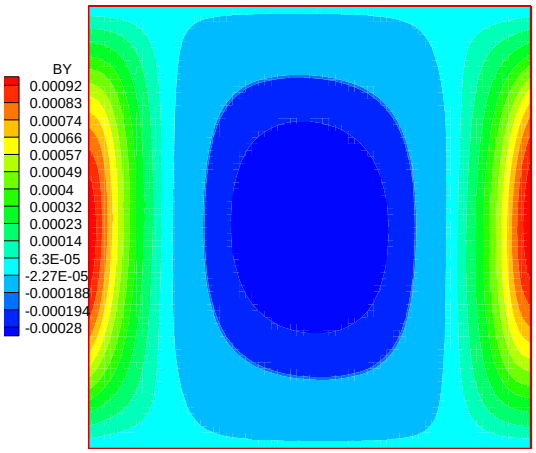


( c)

Fig. 4. Contours of variables: (a) contours of magnetic potential A, (b) contours of magnetic field in the X direction ($B_x$), and (c) contours of magnetic field in the Y direction ($B_y$) at $Re_m=10^{-5}$ and Ha=80

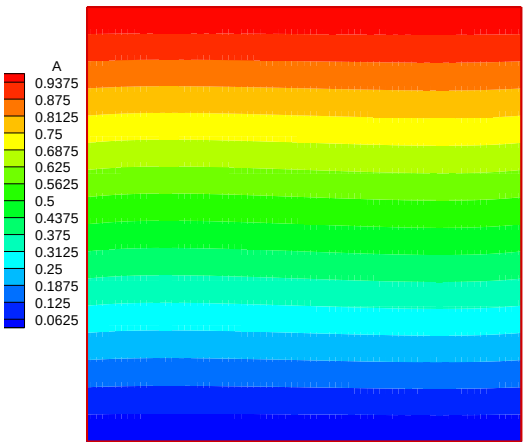


(a)

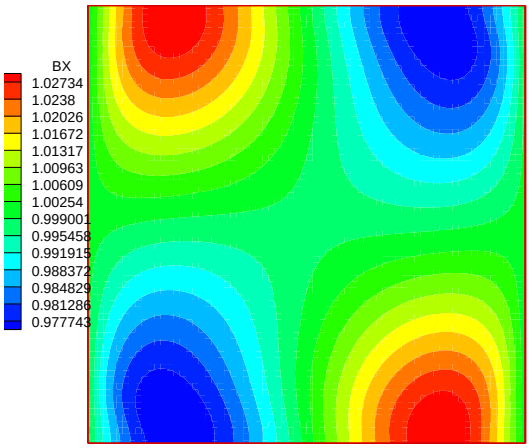


(b)

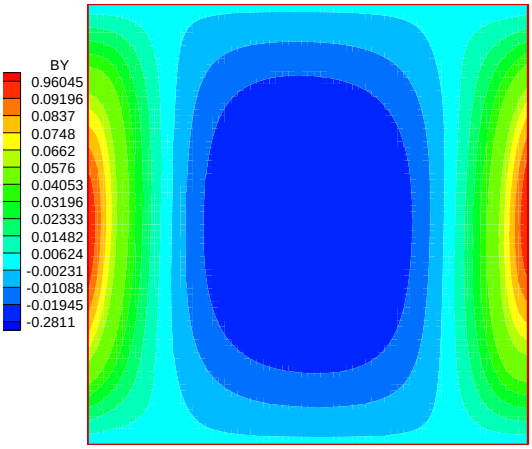


(c)

Fig. 5. Contours of variables: (a) contours of magnetic potential A, (b) contours of magnetic field in the x direction ($B_x$), and (c) contours of magnetic field in the Y direction ($B_y$) at $Re_m=10^{-3}$ and Ha=80

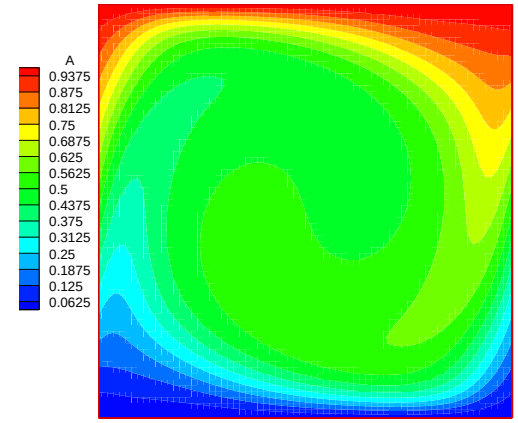


(a)

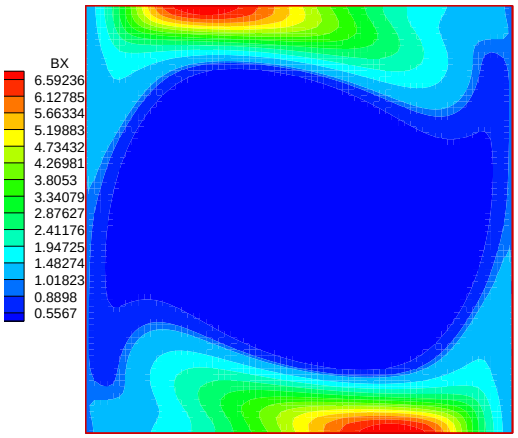


(b)

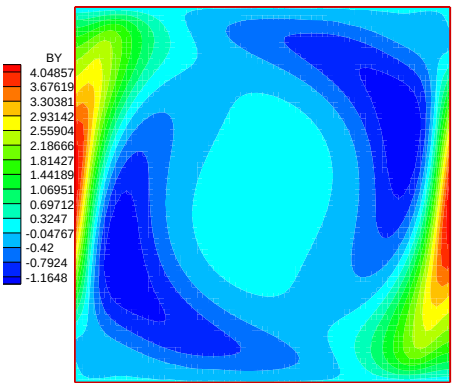


(c)

Fig. 6. Contours of variables: (a) contours of magnetic potential A, (b) contours of magnetic field in the X direction ($B_x$), and (c) contours of magnetic field in the Y direction ($B_y$) at $Re_m=10^{-1}$ and Ha=80

Fig. 7 presents the mid-height velocity profiles at $Ra=10^5$, Ha=80, and different magnetic Reynolds numbers. At $Re_m=0.1$, the maximum velocity near the hot wall was higher than those at $Re_m=10^{-3}$ and $Re_m=10^{-5}$. The magnetic field near the hot wall was weaker than that near the adiabatic walls (Fig. 6(b)); thus, the Lorentz force was very low in these regions.

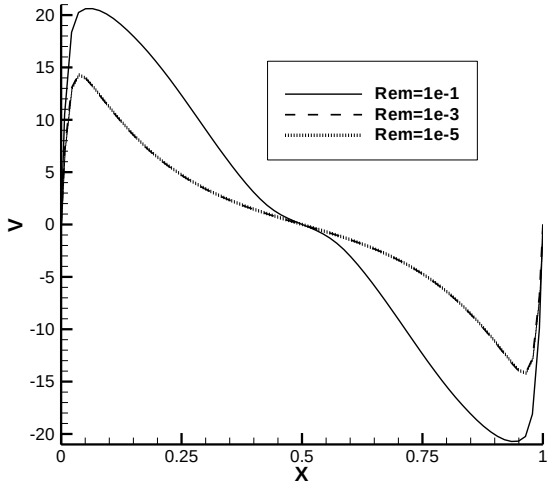


Fig. 7. Velocity profile at $Ra=10^5$, Ha=80, and different magnetic Reynolds numbers

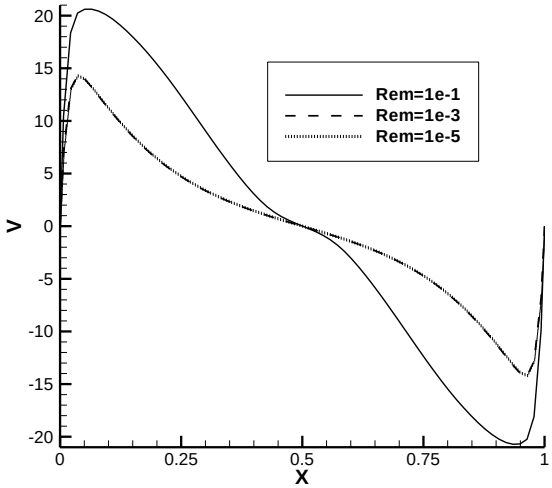


Fig. 8. Temperature velocity profile at $Ra=10^5$, Ha=80, and different magnetic Reynolds numbers

Fig. 8 illustrates the mid-height temperature profiles at $Ra=10^5$, Ha=80, and different magnetic Reynolds numbers. At $Re_m=0.1$, the temperature gradient and the slope of the temperature profile near the hot wall were higher than those at $Re_m=10^{-3}$ and $Re_m=10^{-5}$.

## 6. Conclusion

This study analyzed the steady, laminar, and magneto-convective flow of a viscous fluid in a cavity. Temperature gradient was applied on the two opposing regular walls of the enclosure, whereas adiabatic conditions were maintained in the other walls. A magnetic field was applied in the X direction. Magnetic Reynolds numbers of $10^{-1}$, $10^{-3}$, and $10^{-5}$ were adopted, and the fluid used was liquid sodium with Pr=0.01 and $Ra=10^5$.

As the $Re_m$ increased, the advection of the magnetic potential increased, and variations in the

magnetic field were augmented because fluid flow affected magnetic distribution. The induced magnetic field was negligible, and the magnetic field in the entire cavity was equal to the applied external magnetic field.

## Nomenclature

| | |
|---|---|
| $B_0$ | Magnitude of magnetic field |
| Bx | Magnitude of magnetic field in the X direction |
| By | Magnitude of magnetic field in the Y direction |
| g | Acceleration due to gravity |
| Cp | Heat capacity |
| A | Magnetic potential vector |
| H | Height of enclosure |
| Ha | Hartmann number |
| Ra | Rayleigh number |
| $Re_m$ | Magnetic Reynolds number |
| P | Pressure |
| k | Thermal conductivity |
| T | Temperature |
| u, v | Velocity components |
| $\beta$ | Coefficient of thermal expansion |
| $\alpha$ | Thermal diffusivity |
| $\gamma$ | Dynamic viscosity |
| $\rho$ | Density |
| $\sigma$ | Electrical conductivity |
| $\theta$ | Dimensionless temperature |
| $\mu_0$ | Magnetic permeability |

## References


[1]. G.M. Oreper and J. Szekely, "The effect of an externally imposed magnetic field on buoyancy driven flow in a rectangular cavity", J. Cryst. Growth, 64, 505–515, (1983).

[2]. H. BenHadid, D. Henry, ''Numerical study of convection in the horizontal Bridgman configuration under the action of a constant magnetic field. Part 2. Three-dimensional flow'', J. Fluid Mech., 333, 57–83, (1997).

[3]. R. Bessaiha, M. Kadja, Ph. Marty, ''Effect of wall electrical conductivity and magnetic field orientation on liquid metal flow in a geometry similar to the horizontal Bridgman configuration for crystal growth'', International Journal of Heat and Mass Transfer, 42, 4345-4362, (1999).

[4]. M. Ciofalo and F. Cricchio, ''Influence of a magnetic field on liquid metal free convection in an internally heated cubic enclosure'', International Journal of Numerical Methods for Heat & Fluid Flow, 12(6), 687-715, (2002).

[5]. I.D. Piazza, M. Ciofalo, ''MHD free convection in a liquid metal filled cubic enclosure I. Differential heating'', Int. J. Heat Mass Transfer 45, 1477–1492, (2002).

[6]. I.D. Piazza, M. Ciofalo, ''MHD free convection in a liquid metal filled cubic enclosure II. Internal heating'', Int. J. Heat Mass Transfer 45, 1493–1511, (2002).

[7]. M. Pirmohammadi, M. Ghassemi, ''Effect of magnetic field on convection heat transfer inside a tilted square enclosure'', International Communication in Heat and Mass Transfer, 36, 776–780, (2009).

[8]. M. Pirmohammadi, M. Ghassemi, A. Keshtkar, ''Numerical study of hydromagnetic convection of an electrically conductive fluid with variable properties inside an enclosure'', IEEE Transactions on Plasma Science, 39, 516–520, (2011).

[9]. N.M. Al-Najem, K.M. Khanafer, M.M. El-Rafaee, ''Numerical study of laminar natural convection in tilted enclosure with transverse magnetic field'', Int. J. Numer. Meth. Heat Fluid Flow, 8, 651–672, (1998).

[10]. N. Rudraiah, R.M. Barron, M. Venkatachalappa, C.K. Subbaraya, ''Effect of a magnetic field on free convection in a rectangular enclosure'', Int. J. Eng. Sci., 33, 1075–1084, (1995).

[11]. F. Selimefendigil, H.F. Oztop, K. Al-Salem, Natural convection of ferrofluids in partially heated square enclosures, J. Magn. Magn. Mater., 372, , 122–133, (2014).

[12]. H. Heidary, R. Hosseini, M. Pirmohammadi, M. J. Kermani, ''Numerical study of magnetic field effect on nano-fluid forced convection in a channel'', Journal of Magnetism and Magnetic Matrials, 374, 11-17, (2014).

[13]. N.S. Bondareva, M.A. Sheremet, I. Pop, ''Magnetic field effect on the unsteady natural convection in a right-angle trapezoidal cavity filled with a nanofluid'', Int. J. Numer. Methods Heat. Fluid Flow., 25, 1924–1946, (2015).

[14]. I.V. Miroshnichenko, M.A. Sheremet, H.F. Oztopc, K. A-Salem, ''MHD natural convection in a partially open trapezoidal cavity filled with a nanofluid'', International Journal of Mechanical Sciences, 119, 294–302, (2016).

[15]. P.A. Davidson, ''An Introduction to Magnetohydrodynamics'', Cambridge University Press, Cambridge, 2001.

[16]. U. Müller, L. Bühler, ''Magnetofluiddynamics in channels and containers'', Springer, Wien, New York, (2001).

[17]. S.S. Sazhin, M. Makhlouf, ''Solutions of magnetohydrodynamic problems based on a convectional computational fluid dynamic code'', International Journal for Numerical Methods in Fluids, 21, 433-442, (1995).

[18]. E. Sarris , G. K. Zikos, A. P. Grecos, N.S. Vlachos, "On the Limits of Validity of the Low Magnetic ReynoldsNumber Approximation in MHD Natural-Convection HeatTransfer", Numerical Heat Transfer (Part B), 50, 157-180, (2006).